



Crystal structure and Hirshfeld surface analysis of (Z)-4-(4-hydroxybenzylidene)-3-methylisoxazol- 5(4H)-one. Corrigendum

Wissame Zemamouche,^a Rima Laroun,^b Noudjoud Hamdouni,^{a*} Ouarda Brihi,^a Ali Boudjada^a and Abdelmadjid Debache^b

^aLaboratoire de Cristallographie, Département de Physique, Université Mentouri-Constantine, 25000 Constantine, Algeria, and ^bLaboratoire de Synthèse de Molécules, d'Intérêts Biologiques, Département de Chimie, Université Mentouri-Constantine, 25000 Constantine, Algeria. *Correspondence e-mail: n_hamdouni@yahoo.fr

In the paper by Zemamouche *et al.* [Acta Cryst. (2018), E74, 926–930], there is an error in the name of the first author.

The name of the first author in the paper by Zemamouche *et al.* (2018) is incorrect and should be ‘Wissame Zemamouche’ as given above.

References

Zemamouche, W., Laroun, R., Hamdouni, N., Brihi, O., Boudjada, A. & Debache, A. (2018). *Acta Cryst. E*74, 926–930.



Received 11 January 2018
Accepted 27 May 2018

Edited by P. Bombicz, Hungarian Academy of Sciences, Hungary

Keywords: crystal structure; isoxazole; hydroxybenzylidene; Z configuration; hydrogen bonding; offset π – π interactions; Hirshfeld surface.

CCDC reference: 1845567

Supporting information: this article has supporting information at journals.iucr.org/e

Crystal structure and Hirshfeld surface analysis of (Z)-4-(4-hydroxybenzylidene)-3-methylisoxazol-5(4H)-one

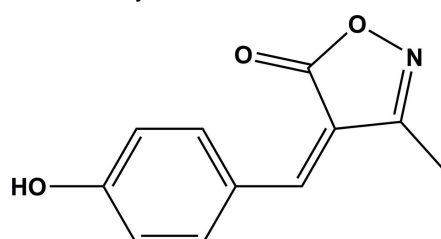
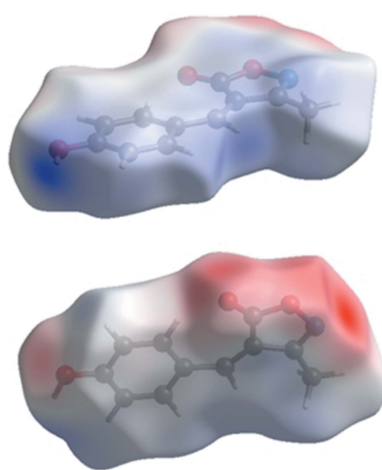
Wissem Zemamouche,^a Rima Laroun,^b Noudjoud Hamdouni,^{a*} Ouarda Brihi,^a Ali Boudjada^a and Abdelmadjid Debache^b

^aLaboratoire de Cristallographie, Département de Physique, Université Mentouri-Constantine, 25000 Constantine, Algeria, and ^bLaboratoire de Synthèse de Molécules, d'Intérêts Biologiques, Département de Chimie, Université Mentouri-Constantine, 25000 Constantine, Algeria. *Correspondence e-mail: n_hamdouni@yahoo.fr

The title compound, $C_{11}H_9NO_3$, contains an isoxazole and a hydroxybenzylidene ring, which are inclined to each other by $3.18(8)^\circ$. There is an intramolecular C–H···O contact forming an $S(7)$ ring. In the crystal, molecules stack head-to-tail in columns along the b -axis direction, linked by offset π – π interactions [intercentroid distances of $3.676(1)$ and $3.723(1)$ Å]. The columns are linked by O–H···O and O–H···N hydrogen bonds, forming layers parallel to the ab plane. The layers are linked by C–H···O hydrogen bonds, forming a supramolecular three-dimensional framework. An analysis of the Hirshfeld surfaces points to the importance of the O–H···O and O–H···N hydrogen bonding in the packing mechanism of the crystal structure.

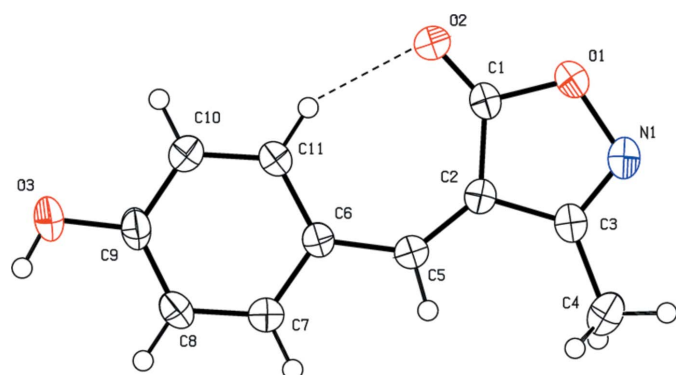
1. Chemical context

The isoxazole ring system is a component of many natural and medicinally active molecules that exhibit interesting biological activities (Wang *et al.*, 2012). Isoxazole derivatives have been shown to possess anticonvulsant (Balalaie *et al.*, 2000), anti-fungal (Santos *et al.*, 2010), HDAC inhibitory (Conti *et al.*, 2010), analgesic (Kano *et al.*, 1967), antimicrobial (Padmaja *et al.*, 2009), antituberculosis (Lee *et al.*, 2009), antimycobacterial (Mao *et al.*, 2010) and many other biological properties. They are also used for the treatment of leishmaniasis (Changtam *et al.*, 2010) and for the treatment of patients with active arthritis (Suryawanshi *et al.*, 2012). Furthermore, the isoxazole unit can be used as the basis for the design and construction of merocyanine dyes, which are used in optical recording and non-linear optical research (Zhang *et al.*, 2011). In the present study, we report on the synthesis, crystal structure and Hirshfeld surface analysis of the title isoxazole derivative.



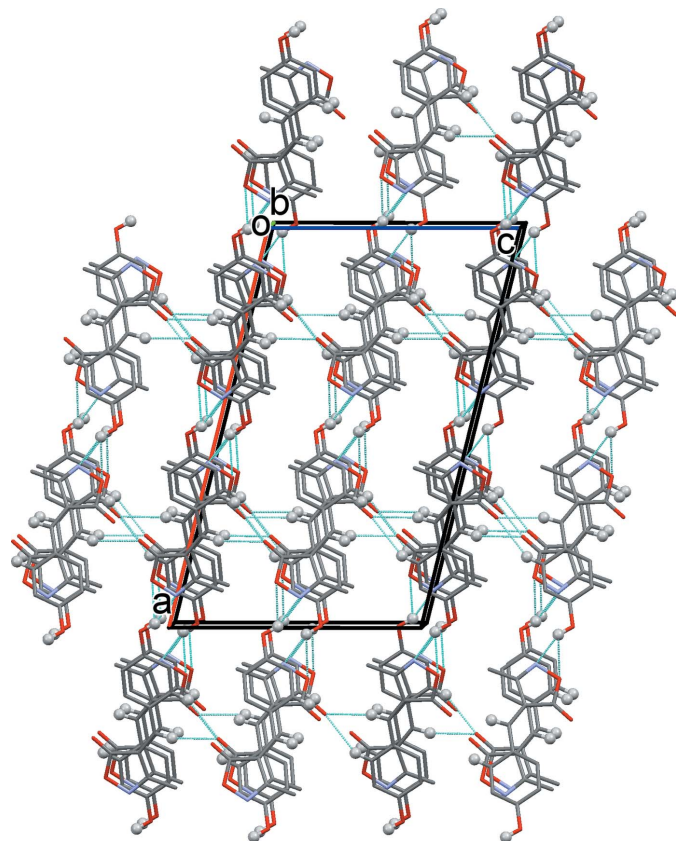
2. Structural commentary

The molecular structure of the title compound is shown in Fig. 1. The molecule is composed of an isoxazole ring (O1/N1/

**Figure 1**

The molecular structure of the title compound, with atom labelling and displacement ellipsoids drawn at the 50% probability level. The intramolecular C—H···O contact (see Table 1) is shown as a dashed line.

C1–C3) that is almost coplanar with the benzene ring (C6–C11) of the 4-hydroxybenzylidene substituent; the two rings are inclined to each other by 3.18 (8)°. The configuration about the C2=C5 bond is Z, and within the molecule there is a short intramolecular C11–H11···O2 contact (Table 1), forming an S(7) ring motif. The bond lengths and bond angles agree well with those observed for a similar compound, the 2-hydroxybenzylidene analogue, (Z)-4-(2-hydroxybenzylidene)-3-methylisoxazol-5(4*H*)-one (Cheng *et al.*, 2009). Here

**Figure 2**

A view along the *b* axis of the crystal packing of the title compound. Only the H atoms (grey balls) involved in hydrogen bonding (see Table 1) have been included.

Table 1
Hydrogen-bond geometry (Å, °).

<i>D</i> —H··· <i>A</i>	<i>D</i> —H	H··· <i>A</i>	<i>D</i> ··· <i>A</i>	<i>D</i> —H··· <i>A</i>
C11—H11···O2	0.93	2.15	2.989 (2)	149
O3—H3O···O1 ⁱ	0.86 (2)	2.41 (2)	2.9119 (18)	118 (2)
O3—H3O···N1 ⁱ	0.86 (2)	2.00 (2)	2.7984 (19)	154 (2)
C5—H5···O2 ⁱⁱ	0.93	2.47	3.3655 (17)	162
C7—H7···O2 ⁱⁱ	0.93	2.55	3.4038 (19)	152

Symmetry codes: (i) $x + \frac{1}{2}, y - \frac{1}{2}, z$; (ii) $x, -y, z - \frac{1}{2}$.

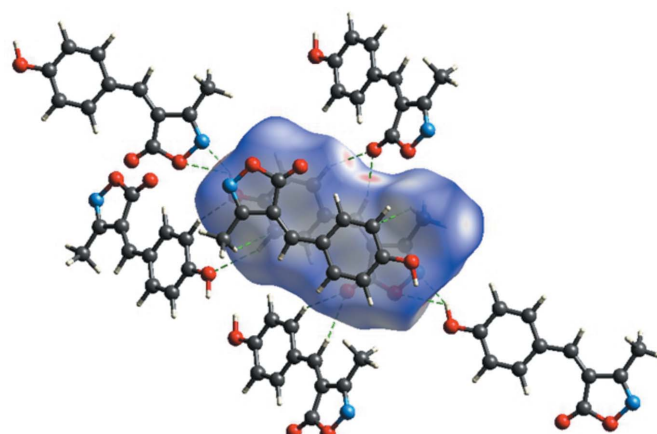
the hydroxyl group is in the *ortho* position, compared to the *para* position in the title compound.

3. Supramolecular features

In the crystal, molecules stack head-to-tail along the *b*-axis direction (Fig. 2), and are linked by offset π – π interactions: $Cg1\cdots Cg2$ ^{iii,iv} intercentroid distances are 3.676 (1) and 3.723 (1) Å, interplanar distances are 3.426 (1) and 3.489 (1) Å, slippages are 1.287 and 1.458 Å with the rings inclined to each other by 3.18 (8)°; symmetry codes: (iii) $-x + \frac{3}{2}, -y + \frac{1}{2}, -z + 1$; (iv) $-x + \frac{3}{2}, -y - \frac{1}{2}, -z + 1$. The molecular columns are linked by O—H···O and O—H···N hydrogen bonds (Table 1), forming layers parallel to (001). The layers are linked by C—H···O hydrogen bonds, forming a supramolecular three-dimensional framework (Table 1 and Fig. 2).

4. Analysis of the Hirshfeld surfaces

Additional insight into the intermolecular interactions was obtained from an analysis of the Hirshfeld surface (Spackman & Jayatilaka, 2009) and the two-dimensional fingerprint plots (McKinnon *et al.*, 2007). The program *CrystalExplorer* (Turner *et al.*, 2017) was used to generate Hirshfeld surfaces mapped over d_{norm} , d_e and the electrostatic potential for the title compound.

**Figure 3**

A view of the Hirshfeld surface mapped over d_{norm} , with neighbouring interactions shown as green dashed lines.

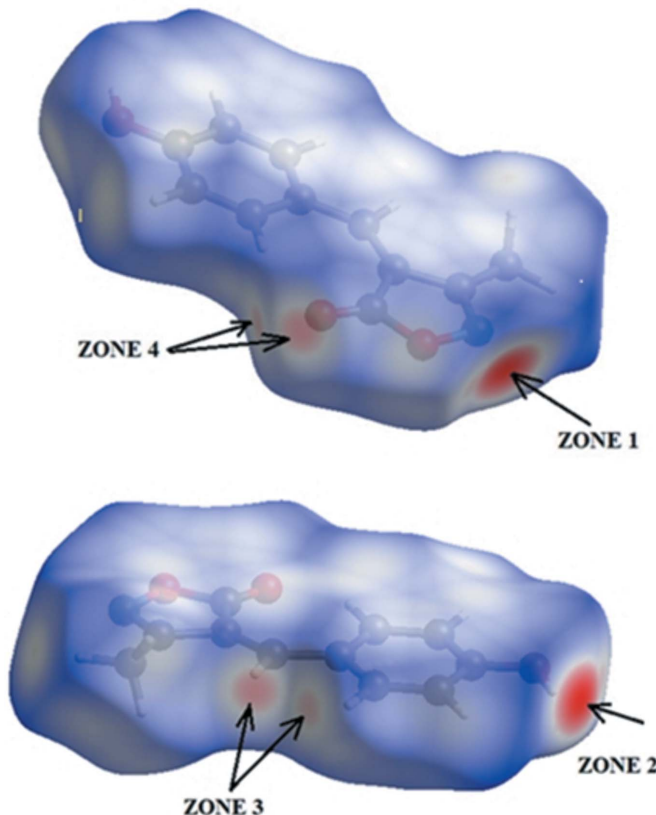


Figure 4
Two views of the Hirshfeld surface mapped over d_{norm} .

The analysis of the Hirshfeld surface mapped over d_{norm} is shown in Fig. 3. The $\text{O}3-\text{H}3\cdots\text{O}1^{\text{i}}$ and $\text{O}3-\text{H}3\cdots\text{N}1^{\text{i}}$ interactions between the corresponding donor and acceptor atoms are visualized as bright-red spots on both sides (zones 1 and 2) of the Hirshfeld surfaces (Fig. 4). Two other red spots exist, corresponding to the $\text{C}5-\text{H}5\cdots\text{O}2^{\text{ii}}$ and $\text{C}7-\text{H}7\cdots\text{O}^{\text{ii}}$ interactions (Fig. 4, zones 3 and 4); these are considered to be weak interactions by comparing them to the sum of the van der Waals radii. The donors and acceptors of intermolecular hydrogen bonds appear as blue and red regions, respectively, around the participating atoms on the Hirshfeld surface mapped over the calculated electrostatic potential (Fig. 5).

The overall two-dimensional fingerprint plot is illustrated in Fig. 6a, and the $\text{H}\cdots\text{O}/\text{O}\cdots\text{H}$, $\text{H}\cdots\text{H}$, $\text{C}\cdots\text{H}/\text{H}\cdots\text{C}$, and $\text{N}\cdots\text{H}/\text{H}\cdots\text{N}$ contacts are illustrated in Fig. 6b–f, respectively. The $\text{H}\cdots\text{O}/\text{O}\cdots\text{H}$ contacts (Fig. 6b) account for 33.9% of the Hirshfeld surface, representing the largest contribution and is displayed on the fingerprint plots by a pair of short spikes at $d_e + d_i = 2.3 \text{ \AA}$. This distance is *ca* 0.5 Å shorter than the sum of the van der Waals radii of the individual atoms, which means it is a very strong interaction. A contribution of 31.0% was found for the interatomic $\text{H}\cdots\text{H}$ contacts (Fig. 6c), with a distinctive peak in the fingerprint plot at $d_e + d_i = 2.2 \text{ \AA}$; the van der Waals radius for this interaction is 2.4 Å. The $\text{H}\cdots\text{C}/\text{C}\cdots\text{H}$ contacts (9.6% contribution; Fig. 6d) are indicated by a pair of short peaks at $d_e + d_i = 2.7 \text{ \AA}$, equal to the sum of the van der Waals radii. The $\text{H}\cdots\text{N}/\text{N}\cdots\text{H}$ contacts (Fig. 6e), which account for only 8.4% of the Hirshfeld surface, are

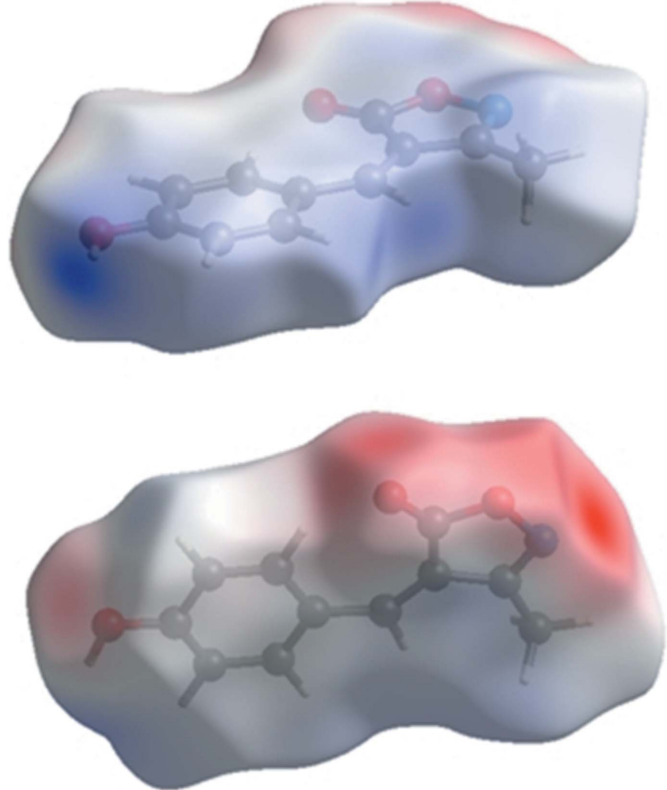


Figure 5
Two views of the Hirshfeld surface mapped over the electrostatic potential.

displayed on the fingerprint plot as a pair of long spikes at $d_e + d_i = 2.0 \text{ \AA}$. This distance differs by *ca* 0.7 Å from the sum of the van der Waals radii, which means it is the strongest interaction present. The $\text{C}\cdots\text{C}$ contacts (Fig. 6f), which account for 11.7% of the Hirshfeld surface with $d_e + d_i = 3.4 \text{ \AA}$, indicate the presence of $\pi\cdots\pi$ stacking.

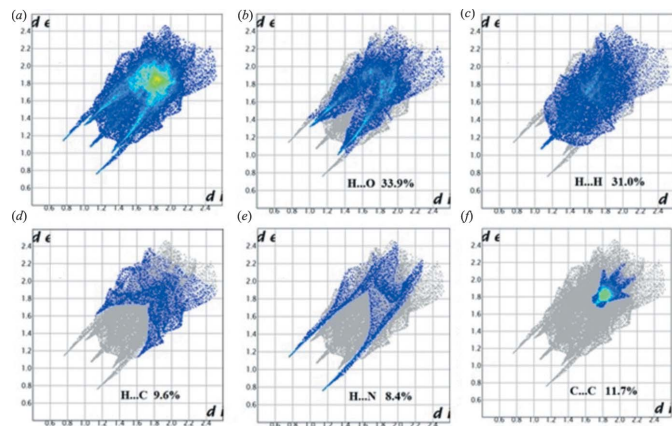


Figure 6
Two-dimensional fingerprint plots: (a) overall, and delineated into contributions from different contacts: (b) $\text{H}\cdots\text{O}/\text{O}\cdots\text{H}$, (c) $\text{H}\cdots\text{H}$, (d) $\text{H}\cdots\text{C}/\text{C}\cdots\text{H}$, (e) $\text{H}\cdots\text{N}/\text{N}\cdots\text{H}$, (f) $\text{C}\cdots\text{C}$.

Table 2
Experimental details.

Crystal data	
Chemical formula	C ₁₁ H ₉ NO ₃
M _r	203.19
Crystal system, space group	Monoclinic, C2/c
Temperature (K)	293
a, b, c (Å)	21.191 (2), 7.2352 (11), 12.9569 (14)
β (°)	103.920 (11)
V (Å ³)	1928.2 (4)
Z	8
Radiation type	Mo Kα
μ (mm ⁻¹)	0.10
Crystal size (mm)	0.36 × 0.23 × 0.11
Data collection	
Diffractometer	Agilent Technologies Xcalibur, Eos
Absorption correction	Multi-scan (<i>CrysAlis PRO</i> ; Agilent, 2013)
T _{min} , T _{max}	0.551, 1.000
No. of measured, independent and observed [I > 2σ(I)] reflections	4536, 1891, 1465
R _{int}	0.021
(sin θ/λ) _{max} (Å ⁻¹)	0.617
Refinement	
R[F ² > 2σ(F ²)], wR(F ²), S	0.040, 0.113, 1.04
No. of reflections	1891
No. of parameters	142
H-atom treatment	H atoms treated by a mixture of independent and constrained refinement
Δρ _{max} , Δρ _{min} (e Å ⁻³)	0.19, -0.13

Computer programs: *CrysAlis PRO* (Agilent, 2013), *SIR92* (Altomare *et al.*, 1994), *PLATON* (Spek, 2009), *Mercury* (Macrae *et al.*, 2008), *SHELXL2018/3* (Sheldrick, 2015) and *publCIF* (Westrip, 2010).

5. Database survey

A search of the Cambridge Structural Database (CSD, V3.59, last update February 2018; Groom *et al.*, 2016) for 4-substituted 3-methyl-isoxazol-5(4H)-ones gave 22 hits. Of these, six compounds involve a benzylidene substituent. The configuration about the C=C bond is Z in all six compounds and the benzene ring is inclined to the isoxazole ring by angles as small as 1.14° in (Z)-4-benzylidene-3-methylisoxazol-5(4H)-one (MBYIOZ01; Chandra *et al.*, 2012) compared to ca 11.59° in (Z)-4-(4-methoxybenzylidene)-3-methyl-1,2-oxazol-5(4H)-one (YIMWIC; Saikh *et al.*, 2013). The most relevant structure is the 2-hydroxybenzylidene analogue, *viz.* (Z)-4-(2-hydroxybenzylidene)-3-methylisoxazol-5(4H)-one (AJESAK; Cheng *et al.*, 2009), in which the two rings are inclined to each other by ca 6.53°, compared to 3.18 (8)° in the title compound. The Z configuration of all six molecules indicates that there is an intramolecular C—H···O contact present forming an S(7) ring motif, as in the title compound (Fig. 1 and Table 1).

6. Synthesis and crystallization

4-Hydroxybenzaldehyde (1 mmol), hydroxylamine hydrochloride (1 mmol), ethylacetacetate (1 mmol) and K₂CO₃ (5 ml) were mixed in a 25 ml flask equipped with a magnetic stirrer. The mixture was refluxed in 5 ml of water for 1 h (the

reaction was monitored by TLC). On completion of the reaction, the mixture was gradually poured into ice-cold water. Stirring was maintained for a few minutes and the obtained solid was filtered and purified by crystallization from ethanol (yield 83%), yielding pale-yellow needle-like crystals on slow evaporation of the solvent.

7. Refinement

Crystal data, data collection and structure refinement details are summarized in Table 2. The hydroxyl H atom was located in a difference-Fourier map and freely refined. The C-bound H atoms were included in calculated positions and treated as riding: C—H = 0.93–0.96 Å with U_{iso}(H) = 1.5U_{eq}(C-methyl) and 1.2U_{eq}(C) for other H atoms.

Acknowledgements

We thank Mr F. Saidi, Engineer at the Laboratory of Crystallography, University Constantine 1, for assistance with the data collection.

Funding information

This work was supported by the Laboratoire de Cristallographie, Department of Physics, Université Constantine 1, Algeria.

References

- Agilent (2013). *CrysAlis PRO*. Agilent Technologies Ltd., Yarnton, England.
- Altomare, A., Cascarano, G., Giacovazzo, C., Guagliardi, A., Burla, M. C., Polidori, G. & Camalli, M. (1994). *J. Appl. Cryst.* **27**, 435.
- Balalaie, S., Sharifi, A. & Ahangarian, B. (2000). *Indian J. Heterocycl. Chem.* **10**, 149–150.
- Chandra, Srikanthamurthy, N., Jeyaseelan, S., Umesha, K. B., Palani, K. & Mahendra, M. (2012). *Acta Cryst.* **E68**, o3091.
- Changtam, C., Hongmanee, P. & Suksamrarn, A. (2010). *Eur. J. Med. Chem.* **45**, 4446–4457.
- Cheng, Q., Xu, X., Liu, L. & Zhang, L. (2009). *Acta Cryst.* **E65**, o3012.
- Conti, P., Tamborini, L., Pinto, A., Sola, L., Ettari, R., Mercurio, C. & De Micheli, C. (2010). *Eur. J. Med. Chem.* **45**, 4331–4338.
- Groom, C. R., Bruno, I. J., Lightfoot, M. P. & Ward, S. C. (2016). *Acta Cryst.* **B72**, 171–179.
- Kano, H., Adachi, I., Kido, R. & Hirose, K. (1967). *J. Med. Chem.* **10**, 411–418.
- Lee, Y. S., Park, S. M. & Kim, B. H. (2009). *Bioorg. Med. Chem. Lett.* **19**, 1126–1128.
- Macrae, C. F., Bruno, I. J., Chisholm, J. A., Edgington, P. R., McCabe, P., Pidcock, E., Rodriguez-Monge, L., Taylor, R., van de Streek, J. & Wood, P. A. (2008). *J. Appl. Cryst.* **41**, 466–470.
- Mao, J., Yuan, H., Wang, Y., Wan, B., Pak, D., He, R. & Franzblau, S. G. (2010). *Bioorg. Med. Chem. Lett.* **20**, 1263–1268.
- McKinnon, J. J., Jayatilaka, D. & Spackman, M. A. (2007). *Chem. Commun.*, pp. 3814–3816.
- Padmaja, A., Payani, T., Reddy, G. D. & Padmavathi, V. (2009). *Eur. J. Med. Chem.* **44**, 4557–4566.
- Saikh, F., Das, J. & Ghosh, S. (2013). *Tetrahedron Lett.* **54**, 4679–4682.
- Santos, M. M. M., Faria, N., Iley, J., Coles, S. J., Hursthouse, M. B., Martins, M. L. & Moreira, R. (2010). *Bioorg. Med. Chem. Lett.* **20**, 193–195.
- Sheldrick, G. M. (2015). *Acta Cryst.* **C71**, 3–8.

- Spackman, M. A. & Jayatilaka, D. (2009). *CrystEngComm*, **11**, 19–32.
- Spek, A. L. (2009). *Acta Cryst. D* **65**, 148–155.
- Suryawanshi, S. N., Tiwari, A., Chandra, N., Ramesh & Gupta, S. (2012). *Bioorg. Med. Chem. Lett.* **22**, 6559–6562.
- Turner, M. J., McKinnon, J. J., Wolff, S. K., Grimwood, D. J., Spackman, P. R., Jayatilaka, D. & Spackman, M. A. (2017). *CrystalExplorer17*. University of Western Australia. <http://hirshfeldsurface.net>
- Wang, L., Yu, X., Feng, X. & Bao, M. (2012). *Org. Lett.* **14**, 2418–2421.
- Westrip, S. P. (2010). *J. Appl. Cryst.* **43**, 920–925.
- Zhang, X. H., Wang, L. Y., Zhan, Y. H., Fu, Y. L., Zhai, G. H. & Wen, Z. Y. (2011). *J. Mol. Struct.* **994**, 371–378.

supporting information

Acta Cryst. (2018). E74, 926-930 [https://doi.org/10.1107/S2056989018007867]

Crystal structure and Hirshfeld surface analysis of (*Z*)-4-(4-hydroxybenzylidene)-3-methylisoxazol-5(4*H*)-one

Wissem Zemamouche, Rima Laroun, Noudjoud Hamdouni, Ouarda Brihi, Ali Boudjada and Abdelmadjid Debache

Computing details

Data collection: *CrysAlis PRO* (Agilent, 2013); cell refinement: *CrysAlis PRO* (Agilent, 2013); data reduction: *CrysAlis PRO* (Agilent, 2013); program(s) used to solve structure: *SIR92* (Altomare *et al.*, 1994); program(s) used to refine structure: *SHELXL2018/3* (Sheldrick, 2015); molecular graphics: *PLATON* (Spek, 2009) and *Mercury* (Macrae *et al.*, 2008); software used to prepare material for publication: *SHELXL2018/3* (Sheldrick, 2015), *PLATON* (Spek, 2009) and *publCIF* (Westrip, 2010).

(*Z*)-4-(4-Hydroxybenzylidene)-3-methylisoxazol-5(4*H*)-one

Crystal data

$C_{11}H_9NO_3$
 $M_r = 203.19$
Monoclinic, $C2/c$
 $a = 21.191 (2)$ Å
 $b = 7.2352 (11)$ Å
 $c = 12.9569 (14)$ Å
 $\beta = 103.920 (11)^\circ$
 $V = 1928.2 (4)$ Å³
 $Z = 8$

$F(000) = 848$
 $D_x = 1.400 \text{ Mg m}^{-3}$
Mo $K\alpha$ radiation, $\lambda = 0.71073$ Å
Cell parameters from 1714 reflections
 $\theta = 4.1\text{--}32^\circ$
 $\mu = 0.10 \text{ mm}^{-1}$
 $T = 293 \text{ K}$
Needle, pale yellow
0.36 × 0.23 × 0.11 mm

Data collection

Agilent Technologies Xcalibur, Eos
diffractometer

4536 measured reflections

Radiation source: Enhance (Mo) X-ray Source

1891 independent reflections

Graphite monochromator

1465 reflections with $I > 2\sigma(I)$

ω scans

$R_{\text{int}} = 0.021$

Absorption correction: multi-scan
(CrysaliPro; Agilent, 2013)

$\theta_{\max} = 26.0^\circ, \theta_{\min} = 3.2^\circ$

$T_{\min} = 0.551, T_{\max} = 1.000$

$h = -26 \rightarrow 23$

$k = -8 \rightarrow 8$

$l = -15 \rightarrow 12$

Refinement

Refinement on F^2

0 restraints

Least-squares matrix: full

Primary atom site location: structure-invariant
direct methods

$R[F^2 > 2\sigma(F^2)] = 0.040$

Secondary atom site location: difference Fourier
map

$wR(F^2) = 0.113$

Hydrogen site location: mixed

$S = 1.04$

1891 reflections

142 parameters

H atoms treated by a mixture of independent and constrained refinement

$$w = 1/[\sigma^2(F_o^2) + (0.0595P)^2]$$

$$\text{where } P = (F_o^2 + 2F_c^2)/3$$

$$(\Delta/\sigma)_{\max} = 0.001$$

$$\Delta\rho_{\max} = 0.19 \text{ e \AA}^{-3}$$

$$\Delta\rho_{\min} = -0.13 \text{ e \AA}^{-3}$$

Extinction correction: (SHELXL-2018/3;

Sheldrick, 2015),

$$Fc^* = kFc[1 + 0.001xFc^2\lambda^3/\sin(2\theta)]^{-1/4}$$

Extinction coefficient: 0.0020 (6)

Special details

Geometry. All esds (except the esd in the dihedral angle between two l.s. planes) are estimated using the full covariance matrix. The cell esds are taken into account individually in the estimation of esds in distances, angles and torsion angles; correlations between esds in cell parameters are only used when they are defined by crystal symmetry. An approximate (isotropic) treatment of cell esds is used for estimating esds involving l.s. planes.

Fractional atomic coordinates and isotropic or equivalent isotropic displacement parameters (\AA^2)

	<i>x</i>	<i>y</i>	<i>z</i>	$U_{\text{iso}}^*/U_{\text{eq}}$
O1	0.62276 (5)	0.14571 (16)	0.60644 (8)	0.0492 (4)
O2	0.72284 (6)	0.0722 (2)	0.69282 (8)	0.0626 (4)
O3	0.99352 (6)	-0.2162 (2)	0.60528 (10)	0.0613 (4)
H3O	1.0132 (11)	-0.237 (3)	0.5558 (16)	0.092 (8)*
N1	0.58554 (6)	0.16143 (18)	0.49783 (10)	0.0448 (4)
C1	0.68443 (8)	0.0886 (2)	0.60805 (12)	0.0392 (4)
C2	0.68735 (7)	0.06174 (19)	0.49745 (11)	0.0308 (3)
C3	0.62309 (7)	0.11381 (19)	0.43784 (12)	0.0347 (4)
C4	0.59837 (9)	0.1192 (2)	0.32016 (13)	0.0521 (5)
H4A	0.558271	0.187052	0.302307	0.078*
H4B	0.591061	-0.004561	0.293277	0.078*
H4C	0.629819	0.178707	0.289026	0.078*
C5	0.73584 (7)	0.00370 (18)	0.45337 (10)	0.0321 (4)
H5	0.723867	0.000592	0.379466	0.039*
C6	0.80178 (7)	-0.05397 (19)	0.49675 (11)	0.0309 (3)
C7	0.83942 (7)	-0.0968 (2)	0.42463 (11)	0.0374 (4)
H7	0.820742	-0.088293	0.352088	0.045*
C8	0.90318 (8)	-0.1508 (2)	0.45834 (12)	0.0407 (4)
H8	0.927260	-0.178127	0.409006	0.049*
C9	0.93153 (7)	-0.1646 (2)	0.56651 (13)	0.0391 (4)
C10	0.89502 (8)	-0.1264 (2)	0.63930 (12)	0.0414 (4)
H10	0.913860	-0.136911	0.711693	0.050*
C11	0.83143 (7)	-0.0732 (2)	0.60553 (11)	0.0374 (4)
H11	0.807415	-0.049326	0.655426	0.045*

Atomic displacement parameters (\AA^2)

	U^{11}	U^{22}	U^{33}	U^{12}	U^{13}	U^{23}
O1	0.0342 (7)	0.0808 (8)	0.0351 (6)	0.0182 (6)	0.0132 (5)	0.0031 (5)
O2	0.0413 (7)	0.1180 (11)	0.0271 (6)	0.0283 (7)	0.0056 (5)	-0.0015 (6)
O3	0.0259 (6)	0.1075 (11)	0.0490 (8)	0.0214 (6)	0.0061 (6)	-0.0077 (7)
N1	0.0290 (8)	0.0631 (8)	0.0410 (8)	0.0122 (7)	0.0057 (6)	0.0029 (6)
C1	0.0271 (8)	0.0580 (9)	0.0335 (8)	0.0104 (7)	0.0091 (7)	0.0017 (7)

C2	0.0256 (8)	0.0372 (7)	0.0289 (7)	0.0031 (6)	0.0050 (6)	0.0010 (6)
C3	0.0274 (8)	0.0405 (7)	0.0363 (8)	0.0049 (7)	0.0076 (7)	0.0005 (6)
C4	0.0392 (10)	0.0710 (11)	0.0397 (9)	0.0134 (9)	-0.0027 (8)	-0.0004 (8)
C5	0.0294 (8)	0.0403 (7)	0.0263 (7)	0.0033 (6)	0.0061 (6)	-0.0002 (6)
C6	0.0258 (8)	0.0373 (7)	0.0297 (7)	0.0036 (6)	0.0067 (6)	-0.0021 (6)
C7	0.0324 (9)	0.0516 (9)	0.0283 (7)	0.0051 (7)	0.0075 (6)	-0.0001 (6)
C8	0.0297 (9)	0.0582 (9)	0.0374 (8)	0.0057 (7)	0.0141 (7)	-0.0051 (7)
C9	0.0225 (8)	0.0503 (9)	0.0435 (8)	0.0067 (7)	0.0062 (7)	-0.0045 (7)
C10	0.0323 (9)	0.0588 (9)	0.0304 (8)	0.0081 (7)	0.0025 (7)	-0.0033 (7)
C11	0.0292 (8)	0.0531 (9)	0.0310 (8)	0.0083 (7)	0.0093 (6)	-0.0032 (6)

Geometric parameters (\AA , $^\circ$)

O1—C1	1.3660 (19)	C5—C6	1.4370 (19)
O1—N1	1.4426 (15)	C5—H5	0.9300
O2—C1	1.2054 (18)	C6—C7	1.401 (2)
O3—C9	1.3417 (18)	C6—C11	1.4053 (19)
O3—H3O	0.86 (2)	C7—C8	1.373 (2)
N1—C3	1.2860 (19)	C7—H7	0.9300
C1—C2	1.462 (2)	C8—C9	1.389 (2)
C2—C5	1.357 (2)	C8—H8	0.9300
C2—C3	1.445 (2)	C9—C10	1.384 (2)
C3—C4	1.489 (2)	C10—C11	1.368 (2)
C4—H4A	0.9600	C10—H10	0.9300
C4—H4B	0.9600	C11—H11	0.9300
C4—H4C	0.9600		
C1—O1—N1	109.59 (11)	C6—C5—H5	113.2
C9—O3—H3O	112.2 (14)	C7—C6—C11	117.27 (13)
C3—N1—O1	107.22 (11)	C7—C6—C5	117.34 (13)
O2—C1—O1	118.53 (14)	C11—C6—C5	125.39 (13)
O2—C1—C2	134.54 (15)	C8—C7—C6	121.68 (13)
O1—C1—C2	106.93 (12)	C8—C7—H7	119.2
C5—C2—C3	124.58 (13)	C6—C7—H7	119.2
C5—C2—C1	131.96 (13)	C7—C8—C9	119.66 (14)
C3—C2—C1	103.46 (13)	C7—C8—H8	120.2
N1—C3—C2	112.79 (13)	C9—C8—H8	120.2
N1—C3—C4	119.70 (14)	O3—C9—C10	117.26 (14)
C2—C3—C4	127.50 (14)	O3—C9—C8	122.99 (14)
C3—C4—H4A	109.5	C10—C9—C8	119.75 (14)
C3—C4—H4B	109.5	C11—C10—C9	120.49 (14)
H4A—C4—H4B	109.5	C11—C10—H10	119.8
C3—C4—H4C	109.5	C9—C10—H10	119.8
H4A—C4—H4C	109.5	C10—C11—C6	121.12 (14)
H4B—C4—H4C	109.5	C10—C11—H11	119.4
C2—C5—C6	133.54 (13)	C6—C11—H11	119.4
C2—C5—H5	113.2		

C1—O1—N1—C3	0.71 (16)	C1—C2—C5—C6	0.4 (3)
N1—O1—C1—O2	178.29 (14)	C2—C5—C6—C7	-176.83 (15)
N1—O1—C1—C2	-1.37 (16)	C2—C5—C6—C11	4.0 (3)
O2—C1—C2—C5	1.7 (3)	C11—C6—C7—C8	-1.6 (2)
O1—C1—C2—C5	-178.74 (15)	C5—C6—C7—C8	179.15 (14)
O2—C1—C2—C3	-178.13 (19)	C6—C7—C8—C9	0.2 (2)
O1—C1—C2—C3	1.45 (16)	C7—C8—C9—O3	-179.90 (15)
O1—N1—C3—C2	0.28 (17)	C7—C8—C9—C10	1.0 (2)
O1—N1—C3—C4	-178.93 (13)	O3—C9—C10—C11	-179.90 (14)
C5—C2—C3—N1	179.09 (14)	C8—C9—C10—C11	-0.7 (2)
C1—C2—C3—N1	-1.08 (17)	C9—C10—C11—C6	-0.7 (2)
C5—C2—C3—C4	-1.8 (2)	C7—C6—C11—C10	1.8 (2)
C1—C2—C3—C4	178.06 (14)	C5—C6—C11—C10	-178.97 (14)
C3—C2—C5—C6	-179.81 (14)		

Hydrogen-bond geometry (Å, °)

D—H···A	D—H	H···A	D···A	D—H···A
C11—H11···O2	0.93	2.15	2.989 (2)	149
O3—H3O···O1 ⁱ	0.86 (2)	2.41 (2)	2.9119 (18)	118 (2)
O3—H3O···N1 ⁱ	0.86 (2)	2.00 (2)	2.7984 (19)	154 (2)
C5—H5···O2 ⁱⁱ	0.93	2.47	3.3655 (17)	162
C7—H7···O2 ⁱⁱ	0.93	2.55	3.4038 (19)	152

Symmetry codes: (i) $x+1/2, y-1/2, z$; (ii) $x, -y, z-1/2$.